

Variation of the cross section for $e^+e^- \rightarrow W^+H^-$ in the Minimal Supersymmetric Standard Model

Heather E. Logan^{1, 2, *} and Shufang Su^{3, †}

¹*Theoretical Physics Department, Fermilab, PO Box 500, Batavia, Illinois 60510-0500, USA*

²*Department of Physics, University of Wisconsin, Madison, Wisconsin 53706, USA*

³*California Institute of Technology, Pasadena, California 91125, USA*

We study the loop-induced process $e^+e^- \rightarrow W^+H^-$ in the Minimal Supersymmetric Standard Model (MSSM). This process allows the charged Higgs boson to be produced in e^+e^- collisions when $e^+e^- \rightarrow H^+H^-$ is kinematically forbidden due to a large charged Higgs mass. We scan over the MSSM parameters subject to experimental constraints to examine the range of values the cross section can take. We find that large enhancements of the cross section over that in a non-supersymmetric two Higgs doublet model are possible, especially for large $\tan\beta$ and light top and bottom squarks. Choosing a few typical MSSM parameter sets, we show the regions in the m_{H^\pm} – $\tan\beta$ plane in which at least 10 $W^\pm H^\mp$ events would be produced at the e^+e^- collider.

PACS numbers: 12.60.Jv, 12.60.Fr, 14.80.Cp, 14.80.Ly

In a recent paper [1] we computed the cross section for $e^+e^- \rightarrow W^+H^-$ in the Minimal Supersymmetric Standard Model (MSSM). This process, which first arises at the one loop level, offers the possibility of producing the charged Higgs boson with mass above half the e^+e^- collider center-of-mass energy \sqrt{s} , when $e^+e^- \rightarrow H^+H^-$ is kinematically forbidden. The cross section for $e^+e^- \rightarrow W^+H^-$ is largest at low values of $\tan\beta$, and can be enhanced over its value in the non-supersymmetric two Higgs doublet model (2HDM) [2, 3] by the contributions of light supersymmetric (SUSY) particles [1]. This is the most promising process considered to date for producing charged Higgs bosons with mass above $\sqrt{s}/2$ in e^+e^- collisions at low to moderate $\tan\beta$ values, above the lower bound of $\tan\beta \geq 2.4$ from the CERN e^+e^- collider LEP-2 Higgs search [4]. This region of low to moderate $\tan\beta$ is exactly where the CERN Large Hadron Collider (LHC) will have difficulty discovering the heavy MSSM Higgs bosons [5, 6, 7].

The goal of this paper is to examine the range of the $e^+e^- \rightarrow W^+H^-$ cross section over the MSSM parameter space, taking into account the present experimental constraints on SUSY particle masses.

The strongest constraint on the MSSM Higgs sector is the lower bound on the mass of the lighter CP-even Higgs boson h^0 from searches at LEP [4]. For given values of m_{H^\pm} and $\tan\beta$, the MSSM prediction for m_{h^0} receives very large radiative corrections of several tens of GeV [8], primarily due to loops involving top quarks and their supersymmetric partners. Obviously, these radiative corrections must be taken into account if the experimental constraint on m_{h^0} is to be used to constrain the MSSM parameter space, and we do so here.

The radiative corrections to the MSSM Higgs sector also appear directly in the calculation of the $e^+e^- \rightarrow$

W^+H^- cross section via the dependence of Feynman diagrams [1, 2] with Higgs bosons in the loop on m_{h^0} and the effective mixing angle α_{eff} , which diagonalizes the CP-even Higgs mass eigenstates and affects the Higgs couplings [9]. Formally, these corrections are of two-loop and higher orders in the cross section; however, because their effects can be large (especially on m_{h^0}), we have examined their impact using the program FeynHiggs [10], which includes the complete one-loop and leading two-loop radiative corrections to the MSSM Higgs boson masses and mixing angle calculated in the Feynman-diagrammatic approach. In fact, we find that the effect on the cross section is quite small, about 5% or less. Nevertheless, we have included these radiative corrections in the numerical results throughout this paper.

We now explore the possible variation of the $e^+e^- \rightarrow W^+H^-$ cross section as a function of the MSSM parameters. The SUSY contributions to this cross section come mainly from loop diagrams involving top and bottom squarks and, to a lesser extent, charginos and neutralinos. The diagrams involving top and bottom squarks are enhanced by the large third-generation Yukawa couplings, but their contribution decouples quickly, like $m_{\tilde{t}, \tilde{b}}^{-2}$, as their masses $m_{\tilde{t}, \tilde{b}}$ increase. The diagrams involving charginos and neutralinos decouple more slowly, like $m_{\tilde{\chi}}^{-1}$, as the relevant chargino or neutralino mass $m_{\tilde{\chi}}$ increases. There are additional contributions from box and t -channel diagrams involving charginos, neutralinos, selectrons, and/or sneutrinos, and from diagrams involving loops of sleptons and of the first two generations of squarks that couple to the charged Higgs boson through the supersymmetric D-terms; however, the contributions of these diagrams are small in general. For explicit expressions, see Ref. [1].

We begin by scanning over the MSSM parameters in the ranges shown in Table I. We use a linear metric for all parameters except $\tan\beta$, for which we use a logarithmic metric. We vary separately the soft SUSY breaking mass M_{SUSY}^{tb} of the top and bottom squarks and the

*Electronic address: logan@pheno.physics.wisc.edu

†Electronic address: shufang@theory.caltech.edu

Parameter	Min	Max
$\tan \beta$	2.4	60
M_{SUSY}^{tb}	50 GeV	1000 GeV
M_{SUSY}	50 GeV	1000 GeV
$ \mu $	50 GeV	1000 GeV
M_1	50 GeV	1000 GeV
M_2	50 GeV	1000 GeV
m_{H^\pm}	$\sqrt{s}/2$	$\sqrt{s} - 100$ GeV

TABLE I: Ranges of SUSY parameters scanned. The μ parameter can take either sign.

$\tilde{\nu}$	$\tilde{\ell}$	\tilde{q}	\tilde{t}_1	\tilde{b}_1	$\tilde{\chi}_1^0$	$\tilde{\chi}_1^\pm$
43 GeV	95 GeV	100 GeV	95 GeV	85 GeV	36 GeV	84.6 GeV

TABLE II: Lower bounds imposed on the SUSY particle masses. \tilde{q} denotes squarks of the first two generations.

mass M_{SUSY} of the sleptons and first two generations of squarks in order to be able to separate the effects of the top and bottom squarks.¹ We take $A_t = A_b = 2M_{\text{SUSY}}^{tb}$, which yields the maximal value for m_{h^0} . The gluino mass enters our calculation only through the two-loop radiative corrections to the Higgs sector and has almost no effect on the cross section; here we set it to 800 GeV.

We discard any points that yield SUSY particle masses below the experimental lower bounds summarized in Table II. These bounds are model dependent; we use the bounds quoted in Ref. [11] for the minimal supergravity scenario, which is reasonable for a large fraction of the scanned parameter space. We also discard any points that give too small a prediction for m_{h^0} . For the large m_{H^\pm} values that we consider, the LEP bound on m_{h^0} coincides with the Standard Model Higgs mass bound of about 114 GeV [12]. After the dominant two-loop radiative corrections to m_{h^0} [10] have been included, the remaining theoretical uncertainty due to uncalculated higher order corrections is estimated to be about ± 3 GeV [13]. We take this into account by lowering the LEP bound by 3 GeV; *i.e.*, we require $m_{h^0} > 111$ GeV. Finally, we discard any points that give too large a SUSY contribution to the ρ parameter [14]; we require $|\Delta\rho_{\text{SUSY}}| < 0.002$ [15].²

¹ A large hierarchy between the masses of the third generation squarks and the first two generations can lead to dangerous flavor changing neutral currents in the B sector only if there are off-diagonal squark mass terms that mix generations. This is strongly dependent on the flavor structure of the model and we do not consider it here.

² In principle, one could also impose the constraints from the measurement of $b \rightarrow s\gamma$, which receives MSSM contributions from diagrams involving charged Higgs boson or chargino exchange, especially at large $\tan \beta$. However, because $b \rightarrow s\gamma$ is a flavor-changing decay, the constraints that it places on the MSSM parameters depend strongly on the presence or absence

The results of the parameter scans are shown in Figs. 1–3. We assume 80% left-polarized electron beams and unpolarized positrons. Where the MSSM cross sections are compared to the 2HDM, we use the MSSM relations for the Higgs masses and mixing angle including radiative corrections in the 2HDM calculation in order to isolate the effects of the SUSY loop diagrams.

In Fig. 1 we compare the cross section in the MSSM with that in the 2HDM as a function of $\tan \beta$, for $\sqrt{s} = 500$ and 1000 GeV. In Fig. 1 only we fix m_{H^\pm} to a single value, $m_{H^\pm} = \sqrt{s}/2$, in order to more clearly illustrate the effect of the MSSM contributions. While the 2HDM cross section falls rapidly with increasing $\tan \beta$, the MSSM contributions depend much more weakly on $\tan \beta$, especially at $\sqrt{s} = 1000$ GeV, where the maximum cross section is almost independent of $\tan \beta$. This implies that the largest relative cross section enhancements due to MSSM contributions occur at large $\tan \beta$, as shown by the different symbols in Fig. 1. At a 500 GeV machine, an enhancement of more than a factor of 10 can occur for $\tan \beta > 10$, while a factor of 100 can occur for $\tan \beta > 40$. At a 1000 GeV machine, the enhancements can be even larger. At low $\tan \beta$, cross section enhancements of roughly 50% are typical.

Assuming an integrated luminosity of 500 fb^{-1} at $\sqrt{s} = 500$ GeV (1000 fb^{-1} at $\sqrt{s} = 1000$ GeV), a cross section above 0.01 fb (0.005 fb) will yield at least $10 W^\pm H^\mp$ events.³ Fig. 1 shows that these cross sections can be reached for most values of $\tan \beta$ thanks to large MSSM enhancements, especially at $\sqrt{s} = 1000$ GeV.

In Fig. 2 we show the cross section (left) and the enhancement relative to the 2HDM (right) as a function of M_{SUSY}^{tb} , for $\sqrt{s} = 500$ GeV. The maximum cross section is roughly independent of M_{SUSY}^{tb} , while the minimum cross section decreases with increasing M_{SUSY}^{tb} . The maximum cross section occurs mainly at small m_{H^\pm} and low $\tan \beta$, for which the 2HDM cross section is already large; SUSY loop contributions yield only a moderate enhancement in this regime. The minimum cross section typically occurs at large $\tan \beta$ when the 2HDM cross section is very small; in this regime large enhancements of the cross section due to top and bottom squark loops occur for low M_{SUSY}^{tb} values, below about 500 GeV. This joint dependence of the enhancement on $\tan \beta$ and M_{SUSY}^{tb} is illustrated in Fig. 3, which shows that large enhancements relative to the 2HDM (triangles and crosses in Fig. 3)

of additional non-minimal flavor structure in the model. Similarly, one could discard any points that yield an unacceptable amount of neutralino dark matter. However, introducing a very small amount of R -parity violation can remove the dark matter constraint while having a negligible effect on the collider phenomenology. In order to maintain generality, then, we have not applied the $b \rightarrow s\gamma$ or dark matter constraints.

³ We choose this 10-event criterion as a measure of the relevance of the $e^+e^- \rightarrow W^+H^-$ production process. We expect that this is too few events to allow a discovery; a background study is needed to establish the minimum observable signal cross section.

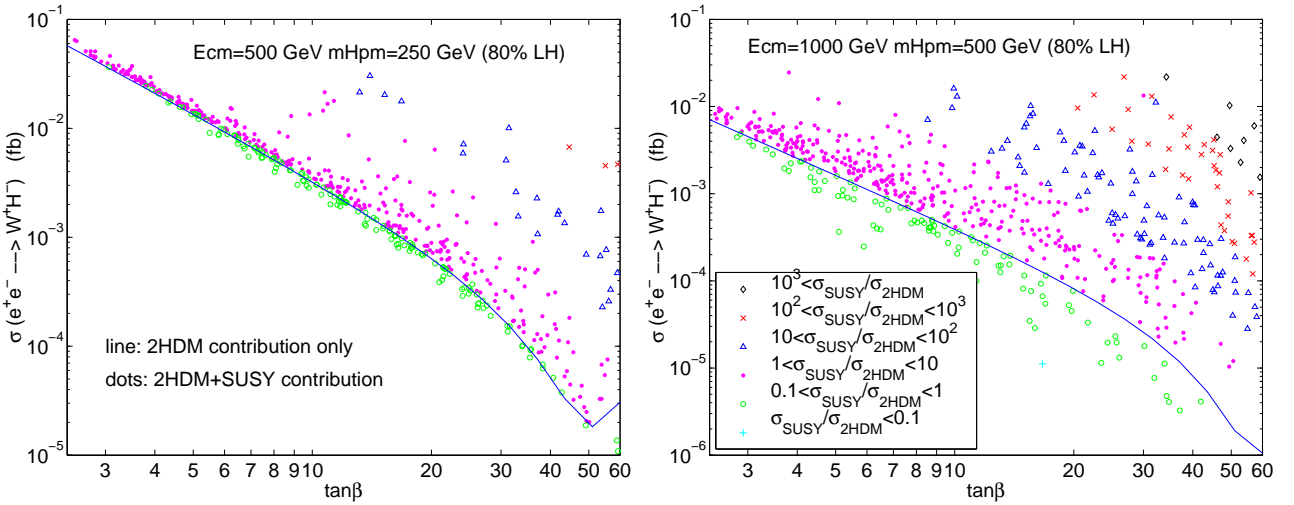


FIG. 1: MSSM cross section as a function of $\tan\beta$ for $\sqrt{s} = 500$ GeV and $m_{H^\pm} = 250$ GeV (left) and $\sqrt{s} = 1000$ GeV and $m_{H^\pm} = 500$ GeV (right). The different symbols show the enhancement of the MSSM cross section relative to the 2HDM. The solid line shows the 2HDM cross section.

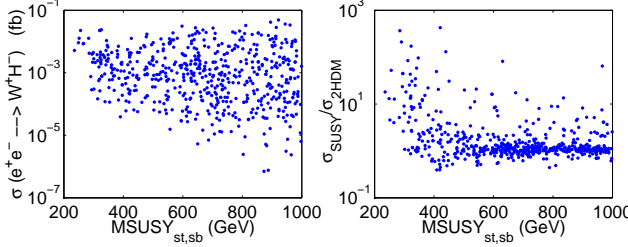


FIG. 2: MSSM cross section (left) and enhancement relative to the 2HDM (right) as a function of $M_{\text{SUSY}}^{\text{tb}}$, for $\sqrt{s} = 500$ GeV.

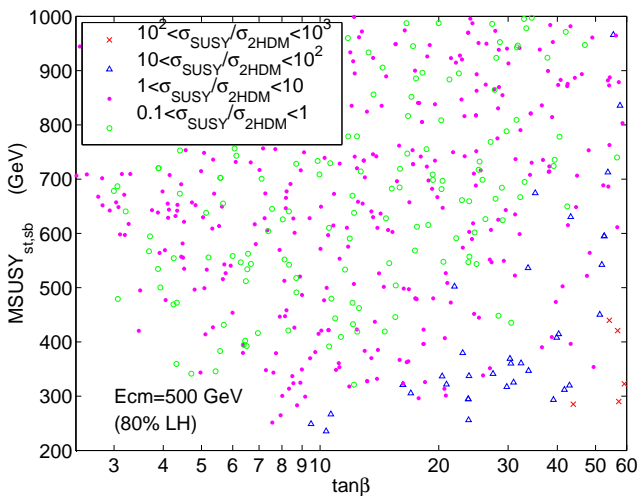


FIG. 3: The MSSM enhancement of the cross section relative to its 2HDM value as a function of $M_{\text{SUSY}}^{\text{tb}}$ and $\tan\beta$, for $\sqrt{s} = 500$ GeV.

require both relatively low $M_{\text{SUSY}}^{\text{tb}}$ and large $\tan\beta$. The situation is similar at $\sqrt{s} = 1000$ GeV.

Finally, the dependence of the cross section on the remaining parameters, M_{SUSY} , μ , M_1 and M_2 , is weaker than the $M_{\text{SUSY}}^{\text{tb}}$ dependence, indicating that the contributions of diagrams involving charginos, neutralinos, sleptons and/or the first two generations of squarks are generally less important than the top and bottom squark contributions.

In order to illustrate the reach of the $e^+e^- \rightarrow W^+H^-$ production process, we choose a “typical” set of SUSY parameters with two values for the μ parameter (see the caption of Fig. 4) that obeys the experimental constraints discussed in the previous section. For this set of parameters, we show contours in Fig. 4 in the m_{H^\pm} – $\tan\beta$ plane below which 10 or more $W^\pm H^\mp$ events will be produced in the e^+e^- collider data sample. As a typical collider run plan, we assume a final integrated luminosity of 500 fb^{-1} at $\sqrt{s} = 500$ GeV and 1000 fb^{-1} at $\sqrt{s} = 1000$ GeV. We plot 10-event contours for the 2HDM⁴ (solid lines) and for the MSSM with $\mu = 200$ GeV (dashed lines) and 500 GeV (dot-dashed lines). We consider an unpolarized e^- beam (light or green lines) and an 80% left-polarized e^- beam (dark or blue lines). In all cases we assume the e^+ beam is unpolarized.

The maximum 10-event reaches in m_{H^\pm} and $\tan\beta$ shown in Fig. 4 are summarized in Table III. In all cases considered, the MSSM contributions increase the 10-event reach over that in the 2HDM: the reach in m_{H^\pm}

⁴ The radiative corrections to the MSSM Higgs boson masses and mixing angle have been included for both the 2HDM and MSSM contours. For the 2HDM Higgs sector radiative corrections we take $\mu = 200$ GeV; taking $\mu = 500$ GeV changes the cross section by less than 1%.

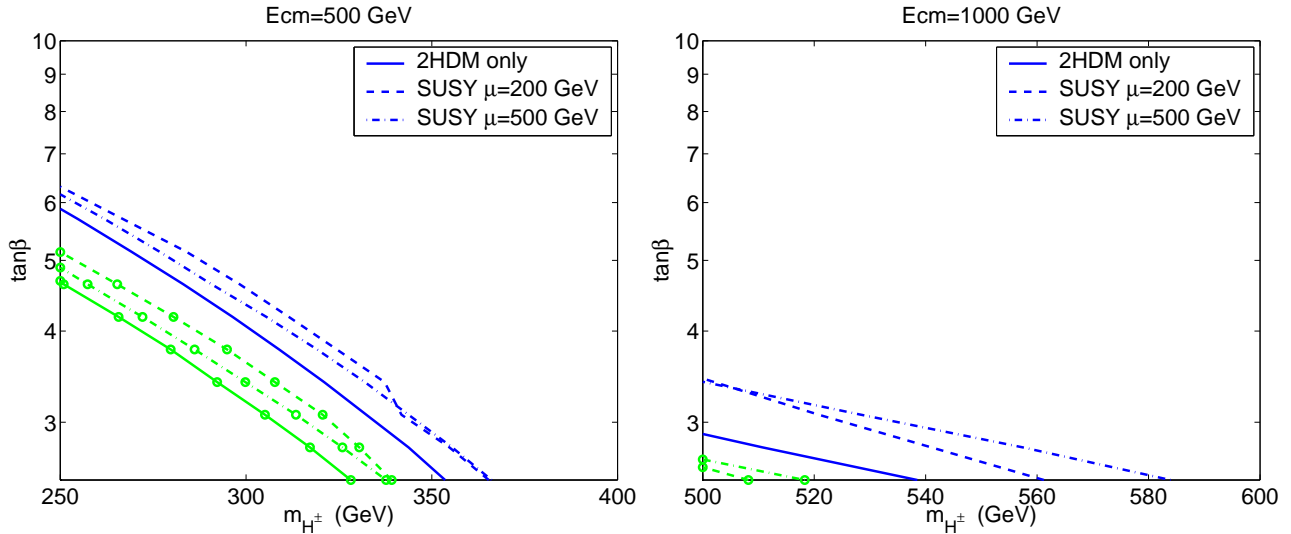


FIG. 4: Ten-event contours for $e^+e^- \rightarrow W^\pm H^\mp$ for $\sqrt{s} = 500$ GeV with 500 fb^{-1} (left) and $\sqrt{s} = 1000$ GeV with 1000 fb^{-1} (right). The SUSY parameters are chosen to be $M_{\text{SUSY}}^{tb} = 1000$ GeV for the top and bottom squarks, $M_{\text{SUSY}} = 200$ GeV for the rest of the squarks and the sleptons, $2M_1 = M_2 = 200$ GeV, $M_{\tilde{g}} = 800$ GeV, $A_t = A_b = 2M_{\text{SUSY}}^{tb}$, and $\mu = 200$ GeV (dashed lines) and 500 GeV (dot-dashed lines). Solid lines show the 2HDM result. Light (green) lines show the cross section and dark (blue) lines show the cross section with an 80% left-polarized e^- beam.

\sqrt{s}	unpolarized		polarized	
	m_{H^\pm}	$\tan\beta$	m_{H^\pm}	$\tan\beta$
$\sqrt{s} = 500 \text{ GeV}$				
2HDM	328 GeV	4.7	354 GeV	5.9
MSSM, $\mu = 200$ GeV	339 GeV	5.1	365 GeV	6.3
MSSM, $\mu = 500$ GeV	338 GeV	4.9	366 GeV	6.2
$\sqrt{s} = 1000 \text{ GeV}$				
2HDM	—	—	539 GeV	2.9
MSSM, $\mu = 200$ GeV	508 GeV	2.6	561 GeV	3.4
MSSM, $\mu = 500$ GeV	518 GeV	2.7	584 GeV	3.4

TABLE III: Maximum 10-event reach in m_{H^\pm} and $\tan\beta$ for the 2HDM and MSSM, from Fig. 4.

is increased by about 10 GeV at $\sqrt{s} = 500$ GeV, and by about 20 GeV or more at $\sqrt{s} = 1000$ GeV. The μ dependence is fairly weak. Using an 80% left-polarized e^- beam increases the reach compared to using unpolarized beams by about 30 GeV in m_{H^\pm} at $\sqrt{s} = 500$ GeV and by twice that at $\sqrt{s} = 1000$ GeV; at either center-of-mass energy the reach in $\tan\beta$ increases by about 1 unit.

To summarize, we examined the range of values for the cross section for $e^+e^- \rightarrow W^+H^-$ possible in the MSSM by scanning over the MSSM parameters, imposing the experimental constraints on the ρ parameter and the masses of the SUSY particles and the lighter CP-even Higgs boson h^0 . While in the 2HDM the cross section falls rapidly with increasing $\tan\beta$, the maximal cross section values in the MSSM are roughly independent of $\tan\beta$, especially at higher collider center-of-mass energies. In particular, very large enhancements of the cross section relative to its value in the 2HDM are possible at large $\tan\beta$. These

large enhancements at large $\tan\beta$ typically occur for low top and bottom squark masses. For low $\tan\beta$, where the 2HDM cross section reaches its maximum value, enhancements of the cross section by about 50% in the MSSM are typical.

We also examined in detail the reach in m_{H^\pm} and $\tan\beta$, focusing on the dependence on the μ parameter and electron beam polarization. Because the cross section is quite sensitive to the SUSY parameters, this process can be used not only to produce H^\pm at low $\tan\beta$, but also to test and/or constrain the MSSM [16].

Finally, we found that using the radiatively corrected MSSM Higgs boson masses and mixing angle in the cross section calculation instead of the tree-level masses and mixing angle has only a small numerical effect on the cross section.

Note added: As we were finishing this paper, we learned about another group [17] working on the same subject.

Acknowledgments

We thank Sven Heinemeyer for many helpful discussions and suggestions. We thank Oliver Brein for comparison of the numerical results. Fermilab is operated by Universities Research Association Inc. under contract no. DE-AC02-76CH03000 with the U.S. Department of Energy. S.S. is supported by the DOE under grant DE-FG03-92-ER-40701 and by the John A. McCone Fellowship.

[1] H. E. Logan and S. Su, Phys. Rev. D **66**, 035001 (2002).

[2] A. Arhrib, M. Capdequi Peyranere, W. Hollik and G. Moultaka, Nucl. Phys. B **581**, 34 (2000); S. Kanemura, Eur. Phys. J. C **17**, 473 (2000).

[3] S. H. Zhu, arXiv:hep-ph/9901221.

[4] LEP Higgs Working Group Collaboration, arXiv:hep-ex/0107030.

[5] K. Lassila-Perini, ETH Dissertation thesis No. 12961 (1998); ATLAS collaboration Technical Design Report, available from <http://atlasinfo.cern.ch/Atlas/GROUPS/PHYSICS/TDR/access.html>.

[6] K. A. Assamagan, Y. Coadou and A. Deandrea, EPJdirect C **09**, 1 (2002);
K. A. Assamagan and Y. Coadou, Acta Phys. Polon. B **33**, 707 (2002).

[7] D. Denegri *et al.*, arXiv:hep-ph/0112045.

[8] For a review and references, see M. Carena, H. E. Haber, S. Heinemeyer, W. Hollik, C. E. Wagner and G. Weiglein, Nucl. Phys. B **580**, 29 (2000).

[9] J. F. Gunion and H. E. Haber, Nucl. Phys. B **272**, 1 (1986) [Erratum-ibid. B **402**, 567 (1993)]; Nucl. Phys. B **278**, 449 (1986); J. F. Gunion, H. E. Haber, G. L. Kane and S. Dawson, *The Higgs Hunter's Guide*, (Perseus Publishing, Cambridge, MA, 2000).

[10] S. Heinemeyer, W. Hollik and G. Weiglein, Comput. Phys. Commun. **124**, 76 (2000); see <http://www.feynhiggs.de>.

[11] S. Ambrosanio, A. Dedes, S. Heinemeyer, S. Su and G. Weiglein, Nucl. Phys. B **624**, 3 (2002).

[12] R. Barate *et al.* [ALEPH Collaboration], Phys. Lett. B **499**, 53 (2001); LEP Higgs Working Group, arXiv:hep-ex/0107029 (LHWG/2001-03).

[13] S. Heinemeyer, W. Hollik and G. Weiglein, Eur. Phys. J. C **9**, 343 (1999).

[14] A. Djouadi, P. Gambino, S. Heinemeyer, W. Hollik, C. Junger and G. Weiglein, Phys. Rev. D **57**, 4179 (1998).

[15] D. E. Groom *et al.* [Particle Data Group Collaboration], Eur. Phys. J. C **15**, 1 (2000), and 2001 partial update for 2002 edition (URL: <http://pdg.lbl.gov>).

[16] The use of a Higgs boson production cross section to constrain the MSSM has also been considered in S. Dawson and S. Heinemeyer, Phys. Rev. D **66**, 055002 (2002).

[17] O. Brein, W. Hollik and T. Hahn, in preparation; O. Brein, arXiv:hep-ph/0209124.